Reconstruction of the flight and attitude of Rosetta's lander Philae

Philip Heinisch, Hans-Ulrich Auster, Dirk Plettemeier, Wlodek Kofman, Alain Herique, Christoph Statz, Ronny Hahnel, Yves Rogez, Ingo Richter, Martin Hilchenbach, et al.

▶ **To cite this version:**

Philip Heinisch, Hans-Ulrich Auster, Dirk Plettemeier, Wlodek Kofman, Alain Herique, et al.. Reconstruction of the flight and attitude of Rosetta's lander Philae. Acta Astronautica, 2017, 140, pp.509-516. ⟨10.1016/j.actaastro.2017.09.017⟩. ⟨insu-03692472⟩

HAL Id: insu-03692472

https://insu.hal.science/insu-03692472v1

Submitted on 18 Aug 2023

HAL is a multi-disciplinary open access archive for the deposit and dissemination of scientific research documents, whether they are published or not. The documents may come from teaching and research institutions in France or abroad, or from public or private research centers.

L'archive ouverte pluridisciplinaire **HAL**, est destinée au dépôt et à la diffusion de documents scientifiques de niveau recherche, publiés ou non, émanant des établissements d'enseignement et de recherche français ou étrangers, des laboratoires publics ou privés.

Distributed under a Creative Commons CC BY-NC-ND 4.0 - Attribution - Non-commercial use - No Derivative Works - International License

Acta Astronautica 140 (2017) 509–516

Contents lists available at ScienceDirect

Acta Astronautica

journal homepage: www.elsevier.com/locate/actaastro

Reconstruction of the flight and attitude of Rosetta's lander Philae

Philip Heinisch [a,*], Hans-Ulrich Auster [a], Dirk Plettemeier [b], Wlodek Kofman [c], Alain Herique [c], Christoph Statz [b], Ronny Hahnel [b], Yves Rogez [c], Ingo Richter [a], Martin Hilchenbach [g], Eric Jurado [d], Romain Garmier [e], Thierry Martin [d], Felix Finke [f], Carsten Güttler [g,a], Holger Sierks [g], Karl-Heinz Glassmeier [a,g]

[a] Institut für Geophysik und Extraterrestrische Physik, Technische Universität Braunschweig, Mendelssohnstrasse 3, 38106, Braunschweig, Germany
[b] Technische Universität Dresden, 01062, Dresden, Germany
[c] Institut de Planetologie et d'Astrophysique de Grenoble, 38041, Grenoble, France
[d] Centre National d'Études Spatiales, 18 Avenue Édouard Belin, 31400, Toulouse, France
[e] CS-SI, Parc de la Plaine, 5 Rue Brindejonc des Moulinais, 31506, Toulouse, France
[f] Center of Applied Space Technology and Microgravity, Am Fallturm 2, 28359, Bremen, Germany
[g] Max-Planck-Institut für Sonnensystemforschung, Justus-von-Liebig-Weg 3, 37077, Göttingen, Germany

ARTICLE INFO

Keywords:
Philae
Rosetta
Attitude
Trajectory
ROMAP
RPC-MAG
CONSERT

ABSTRACT

Since Rosetta's lander Philae touched down on comet 67P/Churyumov-Gerasimenko on November 12, 2014, many tools have been applied to reconstruct Philae's flight path and attitude between separation, the touchdowns, collision and the final landing at Abydos. In addition to images from the cameras onboard both orbiter and lander ("OSIRIS", "CIVA" and "ROLIS"), radio tracking results, solar array and radio data link housekeeping data, one of the major sources for timing and attitude information were two point magnetic field measurements by the magnetometers "ROMAP" and "RPC-MAG" aboard Philae and Rosetta. In this study all the different results are combined to determine in further detail what happened to Philae during its travel above the surface of 67P/Churyumov-Gerasimenko. In addition to a description of the descent dynamics and the attitude during rebound, the approximate coordinates for the collision at 16:20 UTC with the rim of the Hatmehit crater and the second touchdown are estimated. It is also shown, that Philae did not change attitude between the end of the first-science sequence and September 2, 2016.

1. Introduction

In November 2014 Philae landed on comet 67P/Churyumov-Gerasimenko, as part of the Rosetta mission [1–4]. As the Philae lander is not equipped with dedicated navigation instruments [5], information about the trajectory and attitude during descent were to be reconstructed using both orbiter and lander observations. Initially, this was not considered to be problematic, as only a simple gravity based descent without any further movement after touchdown was planned. Several tools were prepared to reconstruct the attitude after landing. Descent tracking would have been possible by analyzing the CONSERT (Comet Nucleus Sounding Experiment by Radiowave Transmission) radio instrument [6] ranging results. Initially the attitude was to be reconstructed primarily using OSIRIS (Optical, Spectroscopic and Infrared Remote Imaging System) camera images taken from orbit and by analyzing the currents of the individual solar cells [7] backed up by the comparison of magnetic two-point observations using the orbiter and lander magnetometers RPC-MAG (Rosetta Plasma Consortium - Magnetometer) [8] and ROMAP (Rosetta Magnetometer and Plasma Monitor) [9]. Due to the failure of the active descent system (cold gas thruster) and harpoons, Philae bounced of the surface several times before coming to a final rest. Therefore no reliable attitude information could be derived solely from OSIRIS images or solar array currents (due to unknown illumination conditions) and the magnetic field measurements became one of the main sources for attitude information.

Instead of just the nominal 7 h descent, it took an additional 2 h (15:34:04 UTC - 17:31:17 UTC) before Philae finally landed [2,7,10,11]. The entire flight is illustrated in Fig. 1 showing the trajectory from the initial touchdown (TD1), collision (COL) and second touchdown (TD2) up to the final touchdown (TD3) overlaid on a mosaic of OSIRIS images of the corresponding area (adapted from Ref. [10]). The coordinates of the individual events were updated using the latest information presented in

* Corresponding author.
E-mail address: p.heinisch@tu-bs.de (P. Heinisch).

https://doi.org/10.1016/j.actaastro.2017.09.017
Received 9 June 2017; Received in revised form 30 August 2017; Accepted 14 September 2017
Available online 19 September 2017
0094-5765/© 2017 The Authors. Published by Elsevier Ltd on behalf of IAA. This is an open access article under the CC BY-NC-ND license (http://creativecommons.org/licenses/by-nc-nd/4.0/).

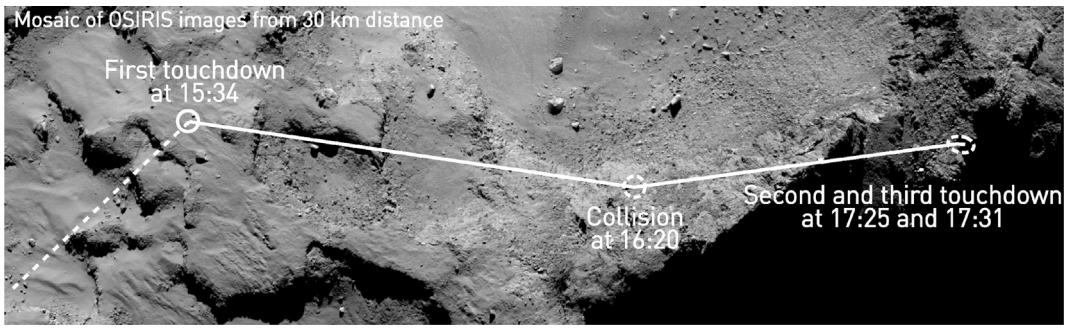

Fig. 1. Philae's trajectory beginning at the descent (dashed white line), showing the first touchdown, the collision, second and third touchdown (white line) overlaid on a mosaic of OSIRIS images taken at a distance of 30 km, adapted from Ref. [10].

this paper and also including TD2. While the locations of TD1 and TD3 are known precisely from OSIRIS and ROLIS images, the coordinates of the collision and the second touchdown were approximated assuming a ballistic trajectory using several different kinds of observations (ranging results, flight times and attitude) [7]. Fortunately, the coordinates of the final landing site (Abydos) became available after Philae was found on OSIRIS images [12].

2. Descent and touchdown 1

On November 12, 2014 at 08:35 UTC Philae was separated from the Rosetta orbiter, descending on a ballistic trajectory towards the surface of comet 67P/Churyumov-Gerasimenko. While the separation and the first touchdown are already well documented [2,7,10,13,14], very little about the descent dynamics and attitude has yet been published [7,15].

Philae was actively stabilized by an internal flywheel during descent. The rotation axis of this flywheel was approximately parallel to the lander z-axis. This ensured accurate antenna pointing and kept the landing gear aligned for touchdown, but allowed Philae to rotate roughly around its z-axis. The rotation rate changed over time due to small changes in the flywheel rotation rate. To accurately reconstruct the descent attitude, these changes in rotation have to be determined.

After separation the CONSERT radio experiment [16] as well as the ROMAP and RPC-MAG sensors were all operating simultaneously. Though the main purpose of the CONSERT instrument operation was to track the distance between Rosetta and Philae during descent, it was also possible to reconstruct the rotation from periodic changes in the CONSERT observations. The concurrent magnetic field measurements could not only be used for scientific purposes [17–20], but also made it possible to reconstruct the dynamic attitude of the lander during descent using a similar approach to the one used by Ref. [21] to reconstruct the final attitude.

2.1. CONSERT observations

CONSERT operated from separation up until 40 min before the nominal time of touchdown [22]. These measurements were performed every 2.5 s. Based on the bi-static CONSERT sounding principle [22], it was possible to track the distance between orbiter and lander through the delay in the direct signal path of the CONSERT received signal. In this data, a modulation of the received signal power (maximum peak power, MPP) in the path between orbiter and lander [23] could be observed. This modulation is a result of the antenna properties (frequency dependent pattern and polarization) of CONSERT lander and orbiter antennas and the movement and changes in attitude of lander and orbiter. It features distinct signal minima which are used to calculate the rotation rate through peak detection using the position of these minima. The temporal distance between two consecutive minima under the assumption that these minima mark the same position in the lander antenna pattern, hence a 360° rotation, yield the rotation rate (see Fig. 2). The measured rotation rate coincides with measurements from other instruments and shows periodic fluctuations and a decline during the descent. This behaviour can also be seen when obtaining the rotation rate from a spectrogram of the maximum peak power measurements (Fig. 3). The differences in rotation rate from the quasi-continuous spectrogram results and from the discrete peak detection results are explained by a method inherent averaging in the spectrogram. The spectrogram was obtained for the whole dataset of 9157 CONSERT measurements during the descent. The temporal window size was chosen to be 1024 measurements as a trade off between frequency resolution (approx. 0.4 mHz) and averaging over time (1024 measurements, correspondent to approx. 43 min. of integration time). The performed FFTs were zero padded to 2^{16} samples yielding a virtual frequency resolution below 0.01 mHz, essentially fine enough to distinguish the observed changes in rotation frequency. The window function was chosen as a Nutall window, which

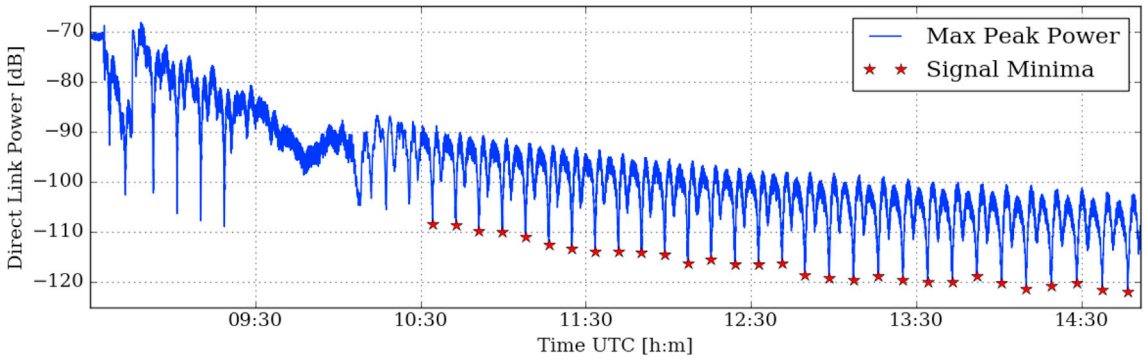

Fig. 2. Maximum peak power of the CONSERT received signal at the orbiter during descent. Detected minima used for the calculation of the rotation rate.

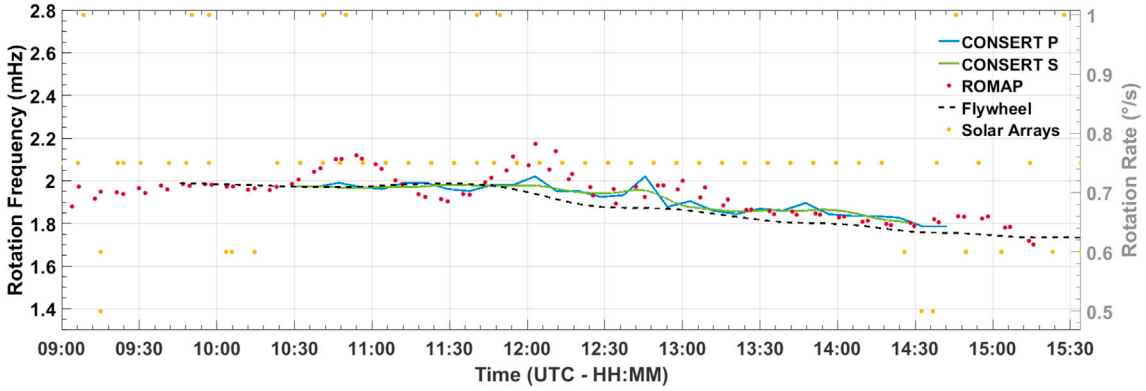

Fig. 3. CONSERT S: Rotation rate from spectrogram of the variation of the signal power during the descent. CONSERT P: Rotation rate from peak detection. Flywheel: Scaled Flywheel rotation rate reconstructed based on ROMAP observations. Solar Arrays: Rotation rate based on solar panel (panel 2 and 4) current fluctuations. ROMAP: Rotation rate reconstructed from magnetic field measurements.

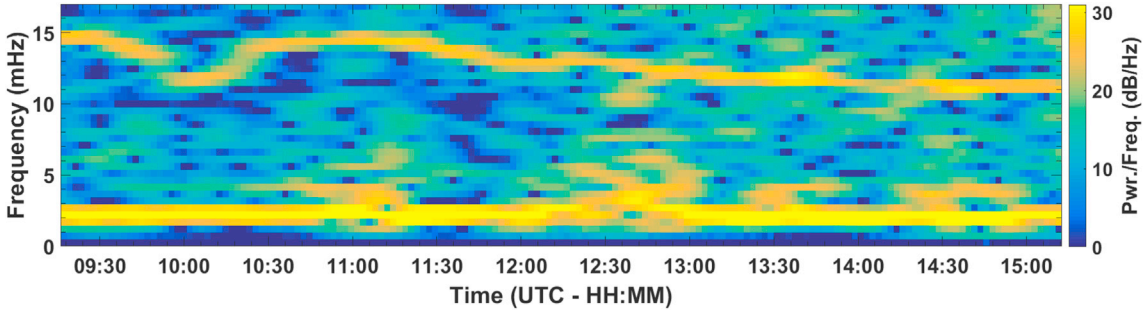

Fig. 4. Dynamic power density spectrum of the Bx-component of the ROMAP magnetic field observations after separation from the orbiter showing two prominent signatures at ∼ 14 mHz and ∼ 2 mHz caused by the flywheel electronics and the lander rotation respectively.

minimizes the FFT artifacts (sidelobes). The rotation frequency hence was extracted from the spectrogram using maximum detection and following of the spectral line corresponding to the approx. 2 mHz or approx. 0.71°/s rotation rate. The results are plotted in comparison to the results obtained by peak detection in Fig. 3. The spectrogram shows the tendency of the rotation behaviour with a temporal resolution of 2.5s. The peak detection indicates the likely true amplitudes of the variation in the rotation rate every ≈ 515s. The CONSERT results are shown in Fig. 3. Fluctuations, especially the increase around 12:30 UTC, can be explained by CONSERT's orbiter antenna properties in conjunction with corrections of the orbiter's attitude during the descent. In order to understand the origin of the observed fluctuations, the radiation and polarization properties of CONSERT's orbiter and lander antennas need to be considered. The CONSERT link characteristic (gain, phase and polarization) between lander and orbiter is a function of the orbiter's attitude. Due to small changes in attitude, the phase property resulting from the antenna-pattern is changed by a large degree. The change in phase yields a change in the polarization angle [23] which causes a variation of the polarization losses and hence the shift of the signal minimum in time. This time shift is observed as fluctuations of the rotation rate.

2.2. RPC-MAG and ROMAP observations

The dynamic power spectrum of the magnetic field observed by ROMAP during descent (see Fig. 4) shows two distinct signatures at ∼14 mHz and ∼2 mHz. While the higher frequency signature was caused by the flywheel electronics, the lower one was directly caused by the lander rotation. The magnetic field created by the high frequency drive circuit of the flywheel motor can be observed in the ROMAP spectrum due to aliasing, even though the ROMAP sampling rate was significantly lower than the flywheel rotation rate. Ground-based tests confirmed that this aliased frequency is proportional to the actual flywheel rotation rate. Therefore, the scaled 14 mHz signature can be used to reconstruct the flywheel rotation. Unfortunately as no usable flywheel housekeeping data is available for the descent period, no direct comparison is possible.

The ROMAP sensor reference frame is aligned with the lander frame (the lander reference frame is shown in Fig. 5). As the alignment of the magnetic axes is known to within 0.6° and the mechanical tolerances are smaller than 1°, the combined alignment error between the two reference frames is below 1.6°. Because of this setup, a rotation around Philae's z-axis causes the observed x- and y- components of the magnetic field to change periodically creating a nearly sinusoidal signature in the observed magnetic field. The frequency is equal to the rate the lander is rotating at. As ROMAP was operating with a sampling rate of 1 Hz, the much slower rotation of Philae was accurately resolved. Fig. 3 shows the reconstructed rotation frequency based on the period of the sinusoidal signatures in the x- and y-components of the ROMAP observations. Additionally, records from two of the solar array currents (solar arrays 2 and 4) were also used to reconstruct the rotation frequency (shown with orange dots) by analyzing the changes in the solar array output current due to the

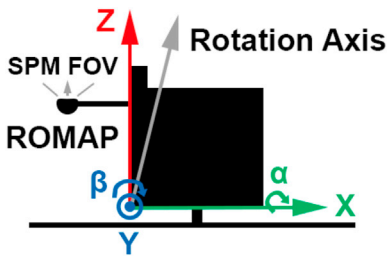

Fig. 5. Illustration of the lander reference frame and rotation axis alignment angles α and β. The ROMAP SPM FOV is indicated by the funnel shaped lines and the arrow above the sensor.

changing insolation patterns. The solar array housekeeping data was sampled every 12 s, therefore the temporal resolution is much worse in comparison to the ROMAP and CONSERT results. The interpretation of the solar array currents is furthermore complicated by geometric influences, for example due to self shadowing. Together with the setup of the lander solar arrays, this makes an unambiguous attitude reconstruction based solely on solar array currents impossible [14]. This however is possible by comparing three-axis magnetic field observations. Still a disadvantage of any reconstruction method based solely on magnetic field measurements is the dependence on the external magnetic field conditions. This can, for example, be seen at around 10:20 UTC and 12:20 UTC were an increase in the overall magnetic activity (see Fig. 4) causes a small apparent increase in the reconstructed rotation frequency while no such change can be observed in the solar array or CONSERT reconstruction. These influences by the external magnetic field could in theory be corrected using orbiter measurements, but this would require knowledge of the lander attitude beforehand to relate the individual magnetic field components. Otherwise, only manual filtering based for example on signatures in the field magnitude can be employed.

The solar array current, CONSERT and ROMAP reconstructions all exhibit a decline in lander rotation rate over time. Based on the ROMAP observations this decrease in the lander rotation frequency seems to be caused directly by a decline in the flywheel rotation frequency. This conclusion can be drawn from the fact that the relative slope of the flywheel signature (see Fig. 4 at approx. 14 mHz) is the same as the one observed in the rotation frequency. As the rotation frequency is already known, only the phase of this rotation, the alignment of the rotation-axis relative to the lander coordinate system and the global alignment of the lander z-axis had to be determined to completely reconstruct the attitude. First, the orientation of the rotation axis relative to the lander z-axis was determined, then in a second step, the phase of the rotation was reconstructed. Finally, the actual orientation of Philae relative to Rosetta was determined.

To ascertain the rough alignment of Philae's rotation axis, the entire three component RPC-MAG timeseries was first transformed into the comet fixed “CHEOPS” coordinate-system (SPICE: 67P/C-GCK) which was selected as global reference. The NASA NAIF SPICE system [24] was used to facilitate the coordinate calculations. Afterwards, the field vectors observed by RPC-MAG were numerically rotated (using the Euler angles α and β) to find the best match between the ROMAP and RPC-MAG z-components similar to what was described by Refs. [21,25]. The resulting rotation matrix describes the transformation necessary to align the z-axis of the CHEOPS system with the z-axis of the lander reference frame. This was possible because Philae was approximately rotating around the lander (and magnetometer) z-axis causing rotation signatures in the x- and y-components, but leaving the ROMAP z-component mostly undisturbed. In a second step the x- and y-component of the ROMAP observations were numerically tilted (using the Euler angles α and β) against the ROMAP z-axis (which is parallel to the lander z-axis) to determine the exact alignment of the rotation axis relative to the lander z-axis. This fine tuning was realized by varying the tilt angles to minimize the power P_z(2 mHz) of the remaining rotational signature in the dynamic power spectrum of the z-component, while simultaneously increasing the correlation with the already roughly aligned RPC-MAG z-observations. These two steps were applied iteratively to maximize the correlation coefficient while decreasing the alignment error. The rotation matrices applied to the RPC-MAG and ROMAP data were of the type:

$$\underline{\underline{M}} = \begin{pmatrix} 1 & 0 & 0 \\ 0 & \cos\alpha & -\sin\alpha \\ 0 & \sin\alpha & \cos\alpha \end{pmatrix} \begin{pmatrix} \cos\beta & 0 & \sin\beta \\ 0 & 1 & 0 \\ -\sin\beta & 0 & \cos\beta \end{pmatrix} \quad (1)$$

The definition of these angles is illustrated in Fig. 5 for the lander case and the results are given in Fig. 6. To resolve temporal changes in the alignment of the rotation axis, the entire interval was split up into 187 individual 20 min segments overlapping each other by 90%. While β remained relatively stable at around $\beta = 10^\circ$, α increased from -10° to 10°, which suggests a small shift in the rotation axis over time. Based on previous work [21,25], an error of approx. $\pm 5^\circ$ can be expected. In a final third step, the phase of the rotation around this axis was determined using a brute-force based approach. The ROMAP magnetic field data (already transformed into a coordinate system where the magnetic z-axis is aligned with the lander rotation axis) was numerically rotated using the previously determined frequency (Fig. 3) while varying the initial rotation phase to get the best match to the corresponding RPC-MAG observations (already transformed into a coordinate system where the magnetic z-axis is aligned with the lander rotation axis). To account for changes in magnetic field conditions, the entire descent interval was split up into sections of 45 min, which were then independently used as input. In contrast to the quasi-static z-axis alignment, the length of the intervals had to be increased from 20 min to 45 min to account for the rotation period. The overlap was kept at 90%. Philae's final attitude was than calculated by combining the rotation in the lander x-y plane with the alignment of the rotation axis relative to the lander z-axis and the alignment of the lander z-axis relative to the CHEOPS reference frame. The detailed attitude results are published in the PSA archive of ESA and the PDS archive of NASA as part of the ancillary mission information [26].

3. Collision

After the first touchdown, Philae lifted off again, and started to spin up, due to the internal flywheel. Even though it was switched off after the touchdown signal was detected by the internal electronics, the flywheel transferred some of its momentum to the lander by internal friction. This spin-up process could accurately be tracked in the spectra of the ROMAP observations, as was done before for the descent. Fig. 7 shows the dynamic power spectral densities for the ROMAP Bx- and Bz- components and overlaid in red the theoretically expected (based on the known moment of inertia of flywheel and lander as described by Ref. [13])

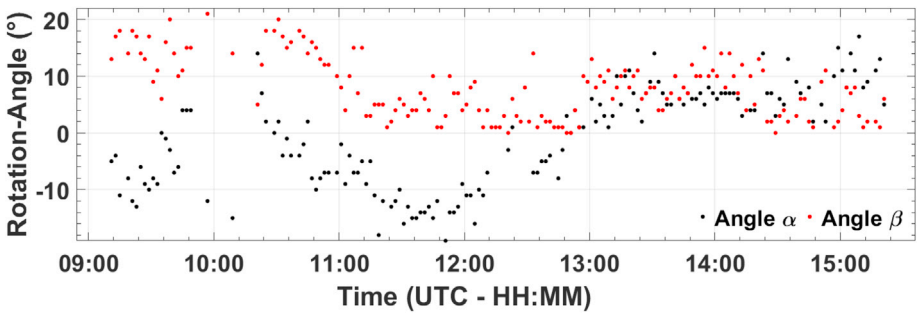

Fig. 6. Rotation angles for the alignment of the lander rotation axis relative to the lander z-axis for individual 20 min intervals overlapping by 90%. Fewer data points are available around 10:20 UTC due to external magnetic field conditions.

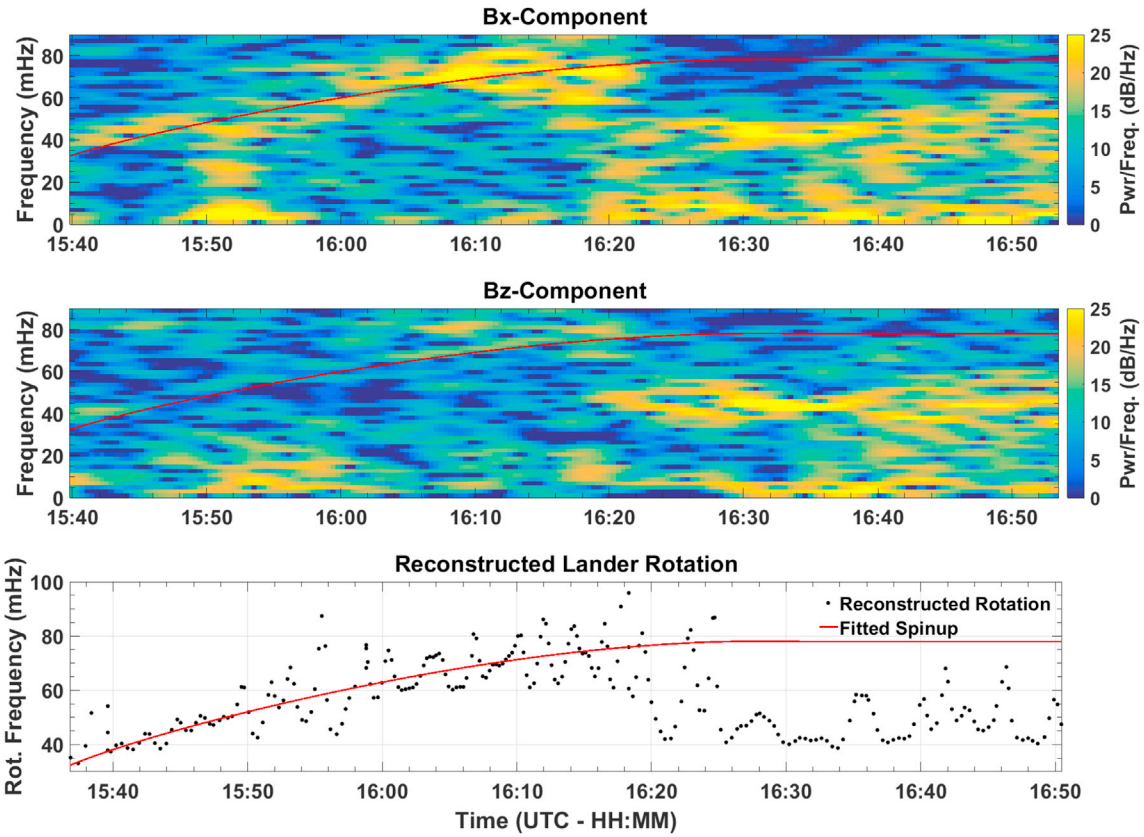

Fig. 7. Dynamic power density spectrum of the Bx- and Bz-components of the ROMAP magnetic field observations after TD1 (15:34 UTC) with the predicted lander rotation frequency (red curve) and the reconstructed rotation frequency (bottom panel). The change in rotation pattern before and after the 16:20 UTC collision event can be seen clearly. The ROMAP By-component was omitted, as it is largely identical to the Bx-component. (For interpretation of the references to colour in this figure legend, the reader is referred to the web version of this article.)

rotation frequency. The bottom panel shows the predicted and reconstructed lander rotation frequency, which reached its maximum of 77 mHz shortly before 16:20:00±1 s UTC. To extract only the lander rotation frequency, a band-pass filter was used to remove all signal components from the timeseries outside the range of 30 mHz–100 mHz (based on the spectra and a comparison with the undisturbed RPC-MAG observations). In a second step, the time between the peaks in the filtered signals was calculated to get the rotation frequency for a given time. Up to 16:20±1*s* UTC the rotation pattern matches the expected curve almost exactly. Afterwards, instead of continuing to spin with a relatively constant frequency (because the flywheel has spun down) as expected, the observed rotation pattern changes drastically and the rotation frequency dropped. This change in rotation pattern was a clear indication that some kind of contact with the surface must have occurred, as there are no possible internal causes for such a drastic tilt. In contrast to the first (and the last two) TDs, no magnetic signature due to ROMAP boom movement was present in the magnetic field observations. This indicates that unlike before, no significant acceleration in the z-direction of the lander was present. Therefore, this event was only classified as a collision with the comet and not as a real touchdown. The approximate geometry of this collision with the rim of the big Hatmehit crater is illustrated in Fig. 8. It is based on the OSIRIS SHAP5 V1.0 [27] digital terrain model (DTM), the reconstructed attitude and the approximate collision coordinates. The attitude was determined from the magnetic field observations, using a similar approach to the descent. First, the alignment of the rotation axis was reconstructed to be able to determine the exact phase of the rotation. To accomplish this, the same approach as previously for the descent was used. As the rotation frequency was already known, only the phase had to be varied and the results compared to the concurrently measured RPC-MAG data. By this means a mean correlation coefficient between all components of > 0.85 was achieved. The coordinates of this collision were based on the trajectory reconstructions done by the SONC Philae flight dynamics team [14,7], taking into account the exact collision time as determined from the ROMAP observations and projecting these results onto the latest OSIRIS DTM. By this means the approximate collision site

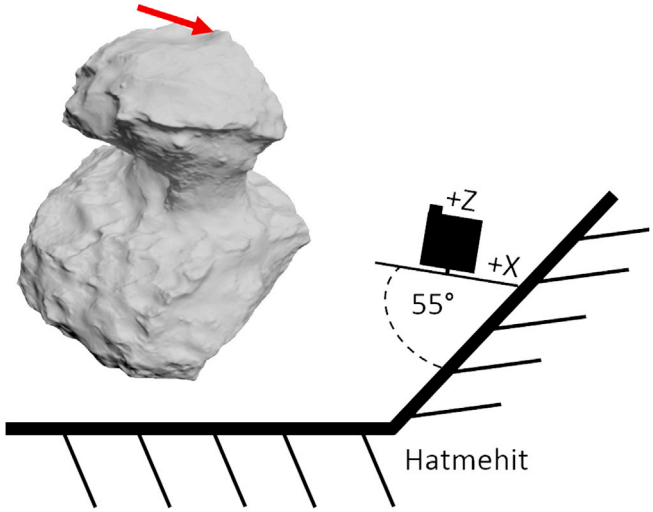

Fig. 8. Illustration of the geometry (not to scale) of the 16:20:00 UTC collision event based on the attitude as reconstructed from ROMAP and RPC-MAG observations. The position of this collision on the comet is shown by the red arrow pointing at the shape model on the left side. (For interpretation of the references to colour in this figure legend, the reader is referred to the web version of this article.)

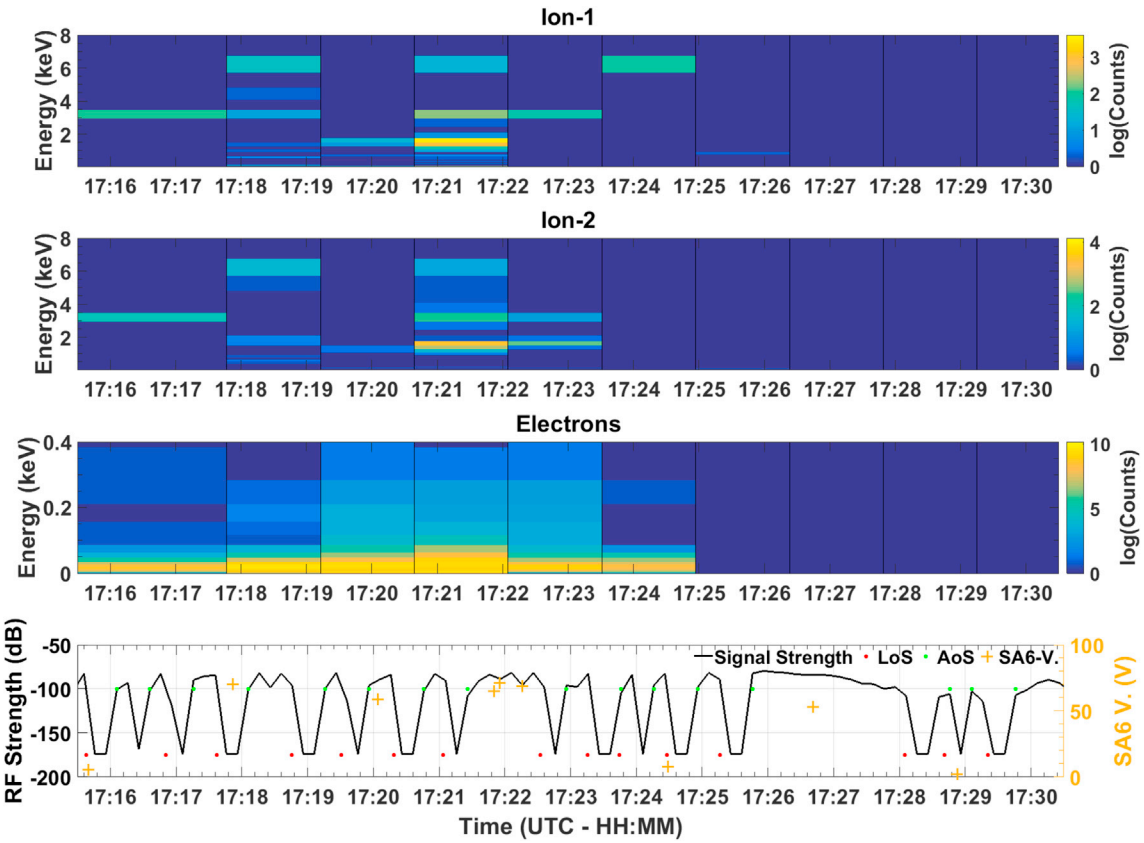

Fig. 9. ROMAP SPM particle counts for the Faraday cup and the two ion-channels showing the sudden drop-out after 17:25 UTC. As comparison the RF-Link signal strength with lander signal acquisition (AoS) and loss off signal (LoS) and the voltage of solar array 6 (SA6) on the lid are displayed.

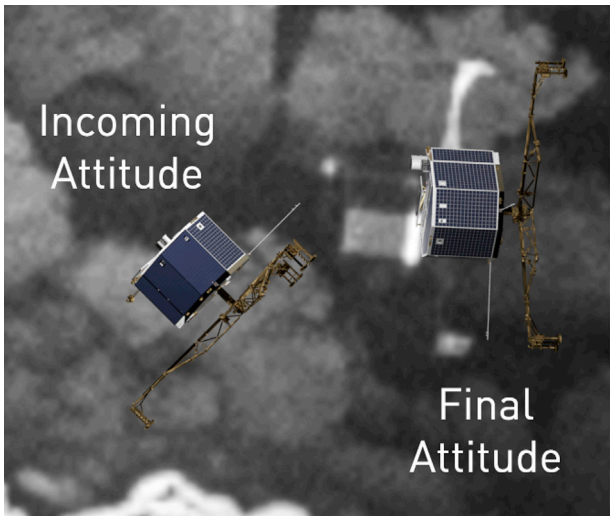

Fig. 10. OSIRIS NAC image of Philae at the final landing site overlaid with two models of Philae illustrating the reconstructed ROMAP attitude before (left) and after TD3 (right - position shifted for visibility). Adapted from Ref. [12].

coordinates were determined to be [2.356; −0.381; −0.121] km using the CHEOPS reference frame. Assuming all these intermediate results to be correct, Philae struck the comet first with the +x-pointing foot with an angle of approx. 55° relative to the surface and a horizontal velocity of approx. 0.23 m/s. This attitude was again checked against the solar array illumination patterns, which confirmed these estimations.

The collision caused Philae's axis of rotation to tilt significantly, while the rotation frequency declined to approx. 42 mHz due to the lost energy. Using the same approach as during the descent to calculate the rotation axis alignment from the magnetic field observations, the new rotation axis was tilted approx. 30° against the lander x-axis and −15° against the y-axis. This tilt in the rotation axis caused the rotation signature to become visible in the spectrum of the ROMAP z-component (see Fig. 7), which is not possible by a simple rotation in the x-y plane (as during descent and before COL). In addition to the rotation, Philae also nutated with a period of 453 s. Because the internal flywheel had completely spun down by 16:20 UTC the dynamic lander attitude was now only governed by its moments of inertia. As this rotation pattern was much more complicated than before the collision, only the attitude directly after the collision and before TD2 was determined. The detailed attitude results are be published in the PSA archive of ESA and the PDS archive of NASA as part of the ancillary mission information [26].

4. Touchdown 2 and touchdown 3

At 17:25:35±1*s* UTC another boom movement was detected in the ROMAP magnetic field observations. Together with a complete change in the dynamic lander attitude after this event, it was a clear indication of another TD, during which Philae lost most of its remaining energy and momentum. Little is known about the details of this 2nd TD as there are no detailed images of the touchdown site. Based on the flight time, surface topography and the known final landing site, this TD most likely happened in the direction of [−0.152; −0.952; 0.266] relative to the final site in an area roughly at [2.445–0.072 −0.343] km in CHEOPS coordinates with a horizontal velocity of approx. 0.16 m/s. Fig. 9 displays the particle counts for the ROMAP plasma monitor SPM (see Fig. 5 for the position of the SPM sensor) ion and electron detectors in addition to RF-Link and solar array housekeeping data. The solar wind particle (ions and electrons) counts drop out immediately after this TD incident and remained zero for the rest of the SPM observation period. As ROMAP HK

remained nominal and the magnetometer continued to operate as expected, mechanical or electrical destruction of the sensor can be excluded. Especially the high-voltage supply needed to operate the SPM deflection plates is known to fail due to arcing if the sensor is compromised in any way.

The top solar array (SA6) was not illuminated at 17:24:30 UTC and moved into sunlight until 17:26:41 UTC. Philae lost the RF-Link with the Rosetta orbiter at 17:25:16 UTC (LoS) and reacquired the signal at 17:25:46 UTC (AoS). Afterwards the link remained stable until 17:28:05 UTC. This behaviour can only be explained by shadowing caused by the surrounding terrain or by Philae pointing away from the sun and the orbiter. Shadowing by terrain is rather unlikely considering the local surface geometry. Based on the earlier behaviour after collision, it is more likely that off-pointing was the cause for the link break and illumination changes. Due to geometric constraints, this would imply that the balcony was pointing in the general direction of the surface. The most likely scenario based on these observations is that the balcony side of the lander with the deployed ROMAP boom tipped towards the comet surface shortly before the time of contact (most likely due to the rotation pattern) and the boom touched the upper surface layers scooping up cometary material that blocked the detector entrances in the process. A dust cloud caused by the surface contact itself would not be sufficient to cover up the SPM sensor, as it was still operating nominally after the much more powerful first TD, which is known to have created a sizable dust cloud [2]. The particle drop-out can also not be caused solely by SPM pointing (i.e. continuously pointing at the surface) because no particles were detected even after the SA6 voltage shows illumination of the panels, which requires the lid (and SPM) to face towards the sun.

After this contact, the attitude of Philae remained relatively stable until it reached its final landing site at 17:31:16±1*s* (based on ROMAP boom movement) UTC after travelling for an additional 6 min and landing at [2.447; −0.063; −0.346] km. The final attitude after TD3 was determined from combined RPC-MAG and ROMAP magnetic field observations [21] with an error below ±5°. This attitude information was successfully used to re-establish contact with Philae in June 2015. Even though the attitude for the time between TD2 and TD3 is only an estimation, it seems plausible based on the local DTM and trajectory, as Philae would have cleared the surrounding terrain during its approach. The translation of the lander was most likely stopped by a cliff-like structure and Philae then touched down with its feet on the comet surface, accelerating the ROMAP boom one last time during TD3. OSIRIS narrow-angle camera (NAC) images taken on September 2, 2016 clearly show Philae at the final landing site [12] and made it possible to accurately determine the landing site coordinates. Fig. 10 shows one of the NAC images overlaid with two rendered models of Philae illustrating the attitude directly before TD3 (left) and the final attitude (right - position shifted for better visibility) the attitude changes commanded at the end of the FSS (translation and rotation [2]) were taken into account to be able to relate the OSIRIS image to the attitude information. These images not only confirm the accuracy of the reconstructed attitude, but also exclude the possibility of any significant attitude change of Philae after the end of the FSS due to outgassing or sublimation.

5. Conclusions

Using several different sources (solar array currents, camera images by OSIRIS, ROLIS & CIVA together with CONSERT radio tracking and ROMAP & RPC-MAG magnetic field observations), it was possible to reconstruct most of Philae's journey above the comet, which was vital for the interpretation of the observational results of the lander. The entire descent was reconstructed, showing a decline in the rotation rate from 2 mHz to 1.7 mHz, while the alignment of the lander z-axis changed by $\sim 10^{\circ}$. After the first touchdown, Philae spun up again (caused by momentum transfer from the flywheel) reaching a maximum rotation frequency of 77 mHz just before it collided with the +x-pointing foot with the rim of the Hatmehit crater (approx. at [2.356; −0.381; −0.121] km) at 16:20 UTC. This surface contact led to a significant tilt in the rotation axis. At 17:25:35 UTC Philae touched down for the second time, which caused the ROMAP magnetometer boom to hit the comet surface. Afterwards, the attitude remained relatively stable until the final touchdown at 17:31:16 UTC ([2.447; −0.063; −0.346] km in CHEOPS reference system). Together with images from orbit and radio-tracking, one of the major sources of this information was magnetic measurements by the ROMAP magnetometer in conjunction with concurrent observations by the magnetometer on the Rosetta orbiter. Knowledge of the final attitude made it possible to predict communication slots and re-establish contact with the lander in June 2015. These results also match the OSIRIS images of Philae and confirm, that Philae's attitude did not change significantly between the end of the FSS in November 2014 and the time the OSIRIS pictures of the lander were taken in September 2016.

Acknowledgements

Rosetta is an ESA mission with contributions from its member states and NASA. We are indebted to the whole Rosetta Mission Team, LCC, SONC, SGS and RMOC for their outstanding efforts making this mission possible. The CONSERT instrument was designed, built and operated by IPAG, LATMOS and MPS and was financially supported by CNES, CNRS, UGA and MPS. The contributions of the CONSERT, ROMAP and RPC-MAG teams were financially supported by the German Ministerium für Wirtschaft und Energie and the Deutsches Zentrum für Luft- und Raumfahrt under contracts 50QP1301 (CONSERT) and 50QP1401 (ROMAP/RPC-MAG). The ROMAP, RPC-MAG and CONSERT data as well as the final attitude/trajectory products will be made available through the PSA archive of ESA and the PDS archive of NASA. The SPICE kernels used for this work are available as ROS-E/M/A/C-SPICE-6-V1.0 through PSA and PDS [26].

References

[1] K.-H. Glassmeier, H. Boehnhardt, D. Koschny, E. Kührt, I. Richter, The rosetta mission: flying towards the origin of the solar system, Space Sci. Rev. 128 (1–4) (2007) 1–21, http://dx.doi.org/10.1007/s11214-006-9140-8. http://dx.doi.org/10.1007/s11214-006-9140-8.

[2] J. Biele, S. Ulamec, M. Maibaum, R. Roll, L. Witte, E. Jurado, P. Muñoz, W. Arnold, H.-U. Auster, C. Casas, C. Faber, C. Fantinati, F. Finke, H.-H. Fischer, K. Geurts, C. Güttler, P. Heinisch, A. Herique, S. Hviid, G. Kargl, M. Knapmeyer, J. Knollenberg, W. Kofman, N. Kömle, E. Kührt, V. Lommatsch, S. Mottola, R. Pardo de Santayana, E. Remetean, F. Scholten, K. Seidensticker, H. Sierks, T. Spohn, The landing(s) of Philae and inferences about comet surface mechanical properties, Science 349 (6247) (2015), http://dx.doi.org/10.1126/science.aaa9816 arXiv: http://www.sciencemag.org/content/349/6247/aaa9816.full.pdf http://www.sciencemag.org/content/349/6247/aaa9816.abstract.

[3] J.-P. Bibring, M.G.G.T. Taylor, C. Alexander, U. Auster, J. Biele, A.E. Finzi, F. Goesmann, G. Klingelhoefer, W. Kofman, S. Mottola, K.J. Seidensticker, T. Spohn, I. Wright, Philae's first days on the comet, Science 349 (6247) (2015) 493, http://dx.doi.org/10.1126/science.aac5116 arXiv: http://science.sciencemag.org/content/349/6247/493.full.pdf http://science.sciencemag.org/content/349/6247/493.

[4] S. Ulamec, M.G. Taylor, Editorial of the special issue-"rosetta and philae at comet 67p/churyumov-gerasimenko", Acta Astronaut. 125 (2016) 1–2. http://dx.doi.org/10.1016/j.actaastro.2016.05.029. http://www.sciencedirect.com/science/article/pii/S0094576516305021.

[5] J.-P. Bibring, H. Rosenbauer, H. Boehnhardt, S. Ulamec, J. Biele, S. Espinasse, B. Feuerbacher, P. Gaudon, P. Hemmerich, P. Kletzkine, D. Moura, R. Mugnuolo, G. Nietner, B. Pätz, R. Roll, H. Scheuerle, K. Szegö, K. Wittmann, The rosetta lander Philae investigations, Space Sci. Rev. 128 (1–4) (2007) 205–220, http://dx.doi.org/10.1007/s11214-006-9138-2. http://dx.doi.org/10.1007/s11214-006-9138-2.

[6] W. Kofman, A. Herique, J.-P. Goutail, T. Hagfors, I. Williams, E. Nielsen, J.-P. Barriot, Y. Barbin, C. Elachi, P. Edenhofer, A.-C. Levasseur-Regourd, D. Plettemeier, G. Picardi, R. Seu, V. Svedhem, The comet Nucleus sounding experiment by Radiowave transmission (CONSERT): a short description of the instrument and of the commissioning stages, Space Sci. Rev. 128 (1–4) (2007) 413–432, http://dx.doi.org/10.1007/s11214-006-9034-9. http://dx.doi.org/10.1007/s11214-006-9034-9.

[7] R. Garmier, T. Ceolin, T. Martin, A. Blazquez, E. Canalias, E. Jurado, E. Remetean, J. Lauren-Varin, B. Dolvies, A. Herique, Y. Roger, W. Kofman, P. Puget, P. Pasquero, S. Zine, L. Jorda, P. Heinisch, Philae Landing on Comet Churyumov-gerasimenko: Understanding of its Descent Trajectory, Attitude, Rebound and Final Landing Site, 2015. ISSFDarXiv: http://issfd.org/2015/files/downloads/papers/083_Garmier.pdf.

[8] K.-H. Glassmeier, I. Richter, A. Diedrich, G. Musmann, U. Auster, U. Motschmann, A. Balogh, C. Carr, E. Cupido, A. Coates, M. Rother, K. Schwingenschuh, K. Szegö, B. Tsurutani, RPC-MAG the fluxgate magnetometer in the ROSETTA plasma Consortium, Space Sci. Rev. 128 (1–4) (2007) 649–670, http://dx.doi.org/10.1007/s11214-006-9114-x. http://dx.doi.org/10.1007/s11214-006-9114-x.

[9] H.-U. Auster, I. Apathy, G. Berghofer, A. Remizov, R. Roll, K. Fornacon, K. Glassmeier, G. Haerendel, I. Hejja, E. Kührt, W. Magnes, D. Moehlmann, U. Motschmann, I. Richter, H. Rosenbauer, C. Russell, J. Rustenbach, K. Sauer, K. Schwingenschuh, I. Szemerey, R. Waesch, ROMAP: rosetta magnetometer and plasma monitor, Space Sci. Rev. 128 (1–4) (2007) 221–240, http://dx.doi.org/10.1007/s11214-006-9033-x. http://dx.doi.org/10.1007/s11214-006-9033-x.

[10] H.-U. Auster, I. Apathy, G. Berghofer, K.-H. Fornacon, A. Remizov, C. Carr, C. Güttler, G. Haerendel, P. Heinisch, D. Hercik, M. Hilchenbach, E. Kührt, W. Magnes, U. Motschmann, I. Richter, C.T. Russell, A. Przyklenk, K. Schwingenschuh, H. Sierks, K.-H. Glassmeier, The Nonmagnetic Nucleus of Comet 67P/Churyumov-gerasimenko, Science (2015), http://dx.doi.org/10.1126/science.aaa5102 arXiv: http://www.sciencemag.org/content/early/2015/04/13/science.aaa5102.full.pdf http://www.sciencemag.org/content/early/2015/04/13/science.aaa5102.abstract.

[11] J.-P. Bibring, M.G.G.T. Taylor, C. Alexander, U. Auster, J. Biele, A.E. Finzi, F. Goesmann, G. Klingelhoefer, W. Kofman, S. Mottola, K.J. Seidensticker, T. Spohn, I. Wright, Philae's first days on the comet, Science 349 (6247) (2015) 493, http://dx.doi.org/10.1126/science.aac5116 arXiv: http://www.sciencemag.org/content/349/6247/493.full.pdf http://www.sciencemag.org/content/349/6247/493.short.

[12] H. Sierks, PHILAE FOUND!, ESA ROSETTA Blog, 2016. http://blogs.esa.int/rosetta/2016/09/05/philae-found/.

[13] R. Roll, L. Witte, Rosetta lander philae: touch-down reconstruction, Planet. Space Sci. 125 (2016) 12–19. http://dx.doi.org/10.1016/j.pss.2016.02.005. http://www.sciencedirect.com/science/article/pii/S0032063315301707.

[14] E. Jurado, T. Martin, E. Canalias, A. Blazquez, R. Garmier, T. Ceolin, P. Gaudon, C. Delmas, J. Biele, S. Ulamec, E. Remetean, A. Torres, J. Laurent-Varin, B. Dolives, A. Herique, Y. Rogez, W. Kofman, L. Jorda, V. Zakharov, J.-F. Crifo, A. Rodionov, P. Heinisch, J.-B. Vincent, Rosetta lander philae: flight dynamics analyses for landing site selection and post-landing operations, Acta Astronaut. 125 (2016) 65–79. http://dx.doi.org/10.1016/j.actaastro.2016.03.030. http://www.sciencedirect.com/science/article/pii/S0094576516302958.

[15] T. Baranyai, A. Balázs, P. L. Várkonyi, Partial Reconstruction of the Rotational Motion of Philae Spacecraft during its Landing on Comet 67P/Churyumov-gerasimenko, ArXiv e-printsarXiv:1604.04414.

[16] Y. Rogez, P. Puget, S. Zine, A. Hérique, W. Kofman, N. Altobelli, M. Ashman, M. Barthélémy, J. Biele, A. Blazquez, C.M. Casas, M.C. Sitjà, C. Delmas, C. Fantinati, J.-F. Fronton, B. Geiger, K. Geurts, B. Grieger, R. Hahnel, R. Hoofs, A. Hubault, E. Jurado, M. Küppers, M. Maibaum, A. Moussi-Souffys, P. Muñoz, L. O'Rourke, B. Pätz, D. Plettemeier, S. Ulamec, C. Vallat, The {CONSERT} operations planning process for the rosetta mission, Acta Astronaut. 125 (2016) 212–233 rosetta and Philae at comet 67P/Churyumov-Gerasimenko, https://doi.org/10.1016/j.actaastro.2016.03.010, http://www.sciencedirect.com/science/article/pii/S0094576516302454.

[17] I. Richter, C. Koenders, H.-U. Auster, D. Frühauff, C. Götz, P. Heinisch, C. Perschke, U. Motschmann, B. Stoll, K. Altwegg, J. Burch, C. Carr, E. Cupido, A. Eriksson, P. Henri, R. Goldstein, J.-P. Lebreton, P. Mokashi, Z. Nemeth, H. Nilsson, M. Rubin, K. Szegö, B.T. Tsurutani, C. Vallat, M. Volwerk, K.-H. Glassmeier, Observation of a new type of low-frequency waves at comet 67P/Churyumov-Gerasimenko, Ann. Geophys. 33 (8) (2015) 1031–1036, http://dx.doi.org/10.5194/angeo-33-1031-2015. http://www.ann-geophys.net/33/1031/2015/.

[18] I. Richter, H.-U. Auster, G. Berghofer, C. Carr, E. Cupido, K.-H. Fornaçon, C. Goetz, P. Heinisch, C. Koenders, B. Stoll, B.T. Tsurutani, C. Vallat, M. Volwerk, K.-H. Glassmeier, Two-point observations of low-frequency waves at 67p/churyumov-gerasimenko during the descent of philae: comparison of rpcmag and romap, Ann. Geophys. 34 (7) (2016) 609–622, http://dx.doi.org/10.5194/angeo-34-609-2016. http://www.ann-geophys.net/34/609/2016/.

[19] K.-H. Glassmeier, Interaction of the solar wind with comets: a rosetta perspective, Philos. Trans. R. Soc. Lond. Math. Phys. Eng. Sci. 375 (2097) (2017), http://dx.doi.org/10.1098/rsta.2016.0256 arXiv:http://rsta.royalsocietypublishing.org/content/375/2097/20160256.full.pdf, http://rsta.royalsocietypublishing.org/content/375/2097/20160256.

[20] P. Heinisch, H.-U. Auster, I. Richter, G. Haerendel, I. Apathy, K.-H. Fornacon, E. Cupido, K.-H. Glassmeier, Joint two-point observations of lf-waves at 67p/churyumov-gerasimenko, Mon. Not. R. Astron. Soc. 469 (Suppl2) (2017) S68, http://dx.doi.org/10.1093/mnras/stx1175. arXiv:/oup/backfile/content_public/journal/mnras/469/suppl_2/10.1093_mnras_stx1175/1/stx1175.pdf. http://dx.doi.org/10.1093/mnras/stx1175.

[21] P. Heinisch, H.-U. Auster, I. Richter, D. Hercik, E. Jurado, R. Garmier, C. Güttler, K.-H. Glassmeier, Attitude reconstruction of rosettas lander {PHILAE} using two-point magnetic field observations by {ROMAPE} and {RPC-MAGE}, Acta Astronaut. 125 (2016) 174–182. http://dx.doi.org/10.1016/j.actaastro.2015.12.002. http://www.sciencedirect.com/science/article/pii/S0094576515004361.

[22] W. Kofman, A. Herique, Y. Barbin, J.-P. Barriot, V. Ciarletti, S. Clifford, P. Edenhofer, C. Elachi, C. Eyraud, J.-P. Goutail, E. Heggy, L. Jorda, J. Lasue, A.-C. Levasseur-Regourd, E. Nielsen, P. Pasquero, F. Preusker, P. Puget, D. Plettemeier, Y. Rogez, H. Sierks, C. Statz, H. Svedhem, I. Williams, S. Zine, J. Van Zyl, Properties of the 67p/churyumov-gerasimenko interior revealed by consert radar, Science 349 (6247) (2015), http://dx.doi.org/10.1126/science.aab0639 arXiv: http://science.sciencemag.org/content/349/6247/aab0639.full.pdf http://science.sciencemag.org/content/349/6247/aab0639.

[23] R. Hahnel, S. Hegler, C. Statz, D. Plettemeier, S. Zine, A. Herique, W. Kofman, {CONSERT} line-of-sight link budget simulator, Planet. Space Sci. 111 (2015) 55–61. http://dx.doi.org/10.1016/j.pss.2015.03.011. http://www.sciencedirect.com/science/article/pii/S0032063315000719.

[24] C.H. Acton, Ancillary data services of NASA's navigation and ancillary information facility, Planet. Space Sci. 44 (1) (1996), 65 – 70, planetary data system, http://dx.doi.org/10.1016/0032-0633(95)00107-7, http://www.sciencedirect.com/science/article/pii/0032063395001077.

[25] P. Heinisch, H.-U. Auster, Determination of variometer alignment by using variation comparison with di3-flux, J. Indian Geophys. Union 19 (4) (2015) 433–446.

[26] J. Vazquez-Garcia, J. Zender, M. Barthelemy, B. Semenov, Rosetta Orbiter/Lander Spice Kernels V1.0, RO/RL-E/M/A/C-SPICE-6-V1.0, 2015. ftp://ssols01.esac.esa.int/pub/data/SPICE/ROSETTA/kernels/.

[27] L. Jorda, R. Gaskell, C. Capanna, S. Hviid, P. Lamy, J. Ďurech, G. Faury, O. Groussin, P. Gutiérrez, C. Jackman, S. Keihm, H. Keller, J. Knollenberg, E. Kührt, S. Marchi, S. Mottola, E. Palmer, F. Schloerb, H. Sierks, J.-B. Vincent, M. A'Hearn, C. Barbieri, R. Rodrigo, D. Koschny, H. Rickman, M. Barucci, J. Bertaux, I. Bertini, G. Cremonese, V.D. Deppo, B. Davidsson, S. Debei, M.D. Cecco, S. Fornasier, M. Fulle, C. Güttler, W.-H. Ip, J. Kramm, M. Küppers, L. Lara, M. Lazzarin, J.L. Moreno, F. Marzari, G. Naletto, N. Oklay, N. Thomas, C. Tubiana, K.-P. Wenzel, The global shape, density and rotation of comet 67p/churyumov-gerasimenko from preperihelion rosetta/osiris observations, Icarus 277 (2016) 257–278. http://dx.doi.org/10.1016/j.icarus.2016.05.002. http://www.sciencedirect.com/science/article/pii/S0019103516301385.